7

Undesirable Radioisotopes Induced by Therapeutic Beams from Medical Linear Accelerators

Adam Konefał
Institute of Physics, Department of Nuclear Physics and Its Application, University of Silesia in Katowice
Poland

1. Introduction

Contemporary linear accelerators called often linacs, used in radiation medicine generate electrons and X-rays with energies up to over 20 MeV. Such energies are enough to induce nuclear reactions in which neutrons and radioisotopes are produced. These neutrons and radioisotopes are undesirable in therapy, because they are source of an additional dose to patients and to staff operating the medical accelerators. The therapeutic electrons and X-rays can induce electronuclear (e,e'n) and photonuclear (γ,n) reactions, respectively. These reactions take place inside the therapeutic beam in massive components of an accelerator head, mainly and in air. In the case of the X-rays the main neutron sources are the collimators of the beam, flattening filter giving the appropriate profile of the beam and the target in which electrons are converted into X-ray radiation. In the case of the electron beams the majority of neutrons are produced in the collimator system and in the scattered foils. The neutrons originated in both mentioned type of reactions have the broad energy spectrum with the high-energy end of more than ten MeV. Majority of the neutrons reach the concrete walls, ceiling and floor of the radiotherapy facility. Concrete is a good moderator. In this medium the neutrons undergo elastic collisions with nuclei of hydrogen, mainly. The slowed down neutrons may get out of concrete and return to air, contributing to the specific distribution of neutron energy inside the radiotherapy facility. Kinetic energies of the slowed down neutrons are distributed according to the Maxwell-Boltzmann distribution law. The neutrons can easy induce the simple capture (n,γ) reactions in the thermal and resonance energy range and radioisotopes are produced. The neutron field is almost uniform in whole accelerator room. Thus the radioisotopes originating from the neutron reactions can be produced in the accelerator components and accessories as well as in the wall, ceiling and floor of the radiotherapy facility. Moreover, the neutrons can induce simple capture reactions in the entrance door of the radiotherapy facility. The penetrative gammas are emitted as a result of these neutron reactions. Therefore, the gamma radiation can appear close to the radiotherapy facility door in the operator room during emission the high-energy therapeutic beams.

In the paper the radioisotopes originating in the accelerator components and in the accessories as well as in the walls, ceiling, floor and door of the radiotherapy facility and in

air are identified for the typical commercial linacs used in European oncological centres. Knowledge of the radioisotopes originating during radiotherapy by the high-energy electron and X-ray therapeutic beams is very significant for the radiological protection of staff operating accelerators as well as for constructors of medical linacs.

2. Characteristic of photonuclear, electronuclear and simple capture reactions

In this paragraph a short characteristic of photonuclear, electronuclear and simple capture reactions will be presented. The dependences between the cross sections and energies of gammas, electrons and neutrons are presented. All cross sections presented in this chapter are taken from web retrieval system of National Nuclear Data Center in Brookhaven National Laboratory, basing on various data base.

2.1 Photonuclear reactions - (γ,n)

Gammas with energy of more than ten MeV are produced mainly in accelerators. Such generated gamma radiation is often called X-rays (bremsstrahlung) and it comes into existence when accelerated electrons are slow down in the force field of the atomic nuclei in a target. The gamma radiation produced in an accelerator is characterized by a spectrum with a continuous distribution of energies. The maximum energy E_{max} of the spectrum corresponds to maximum energy of electrons hitting a target. The high-energy gammas generated by accelerators can induce photonuclear reactions – (γ,n), (γ,2n) and (γ,p). The gamma gives its energy to a nucleus in this interaction. The delivered energy must be at least as great as the binding energy of a neutron or proton in order to eject them from a nucleus in a target. However, separation of a neutron is more probably than separation of a proton because it has no charge contrary to a proton that additionally has to pass through a coulomb barrier of a nucleus. Thus, in a photonuclear reaction a nucleus changes into the other with less a mass number. For heavy nuclei the production of two neutrons in the photonuclear reaction - (γ,2n) is also possible. However, separation of two neutrons needs more photon energy. Energy threshold of the two neutron production is usually near the high-energy end of the therapeutic X-ray beam spectrum. The photonuclear cross section has a resonance character. The maximum value of the cross section depends on the atomic number. It is in the range from several milibarns for light nuclei to several hundred milibarns for heavy nuclei. Moreover, the maximum of the photonuclear cross section corresponds to gamma energy of about 22 MeV for light nuclei and it shifts to about 12 MeV as the atomic number increases. The energy threshold of the photonuclear reactions is about 8 MeV to 10 MeV for most isotopes. In Figure 2.1 the energy spectrum of gamma radiation produced in a medical linear accelerator working in a mode with nominal potential of 20 MV is compared with the photonuclear cross sections for chosen materials.

2.2 Electronuclear reactions - (e,e'n)

Electrons with energies of several MeV or greater can induce electronuclear reactions – (e,e'n). This interaction is an inelastic scattering of an electron in the force field of the atomic nuclei. An electron gives a part of its energy to a nucleus. This energy is partially used to separate a neutron from a nucleus and it is partially change into a kinetic energy of the separated neutron. The cross sections of electronuclear reactions increase with an increasing

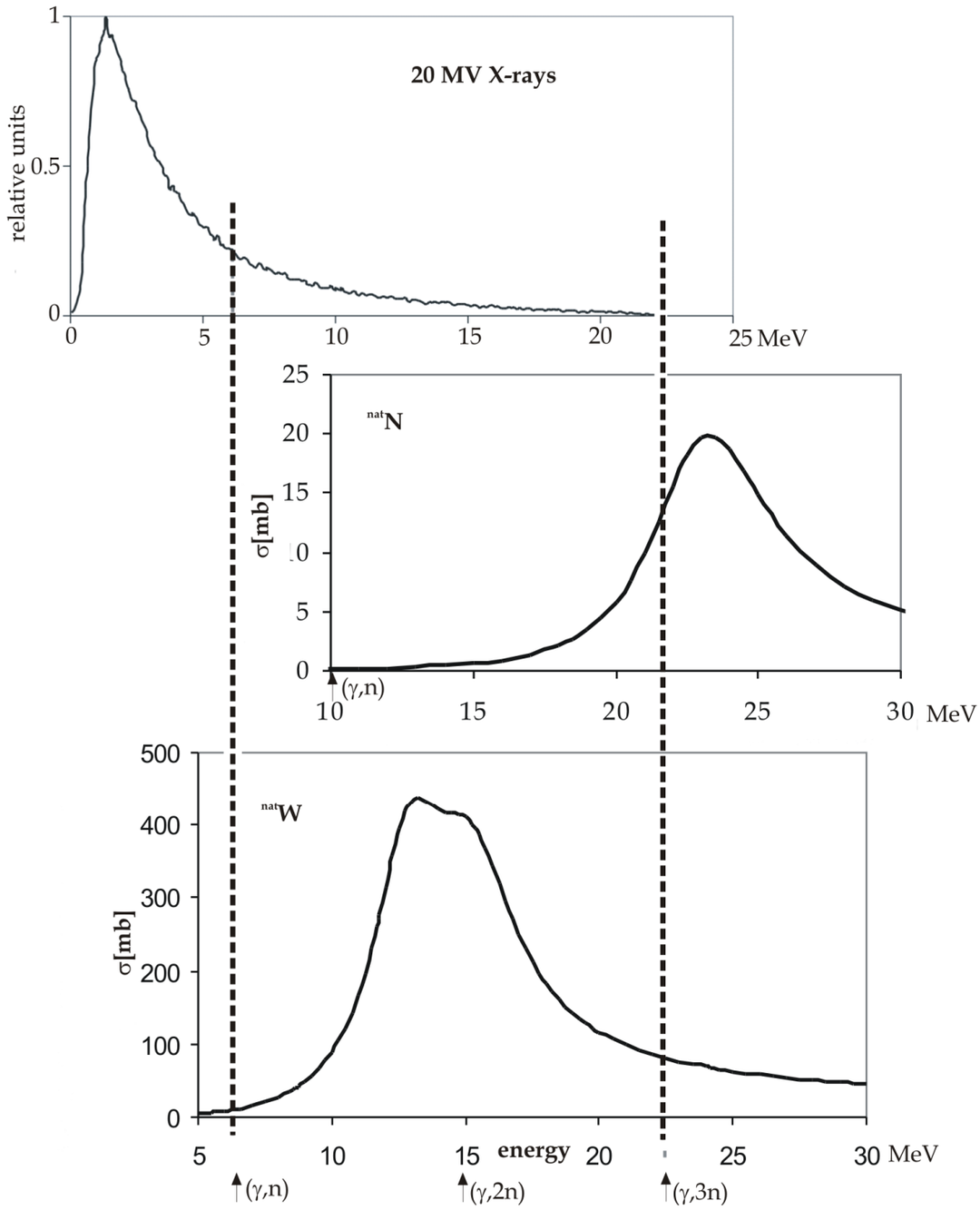

Fig. 2.1. Comparison between the energy range of spectrum of therapeutic 20 MV X-rays and the energy ranges of the photonuclear cross section [12] for natural nitrogen and tungsten. The presented 20 MV X-ray spectrum was derived by the use of Monte Carlo calculation based on the GEANT4 code.

energy of electrons. The neutron production yield in the (e,e'n) reactions is much less than in the case of the (γ,n) reactions. The cross sections of electronuclear reactions are about 3 orders of magnitude less than those for photonuclear reactions in the energy range of the therapeutic beams generated by medical accelerators.

2.3 Simple capture reactions - (n,γ)

Thermal and resonance neutrons can be captured by an atomic nucleus during interaction between a neutron and a nucleus. A photon is emitted by a nucleus as a result of this interaction. Energy of the photon Eγ is equal to $\Delta m \cdot c^2$, where Δm (= M_{neut} + M_{nuc} - M'_{nuc}) is the difference between the sum of the masses of the neutron M_{neut} and the nucleus M_{nuc} before the neutron capture and the mass of the nucleus M'_{nuc} after the neutron capture, c is the velocity of light. Therefore Eγ is called binding energy of a neutron. The (n,γ) reaction can be induced by thermal neutrons for nearly all isotopes. It can also occur in the resonance neutron energy range where the cross sections of the neutron capture reactions have the high peaks (resonance peaks) for a number of isotopes. The cross sections of simple capture reactions as a function of neutron energy for the chosen isotopes are presented in Figure 2.2.

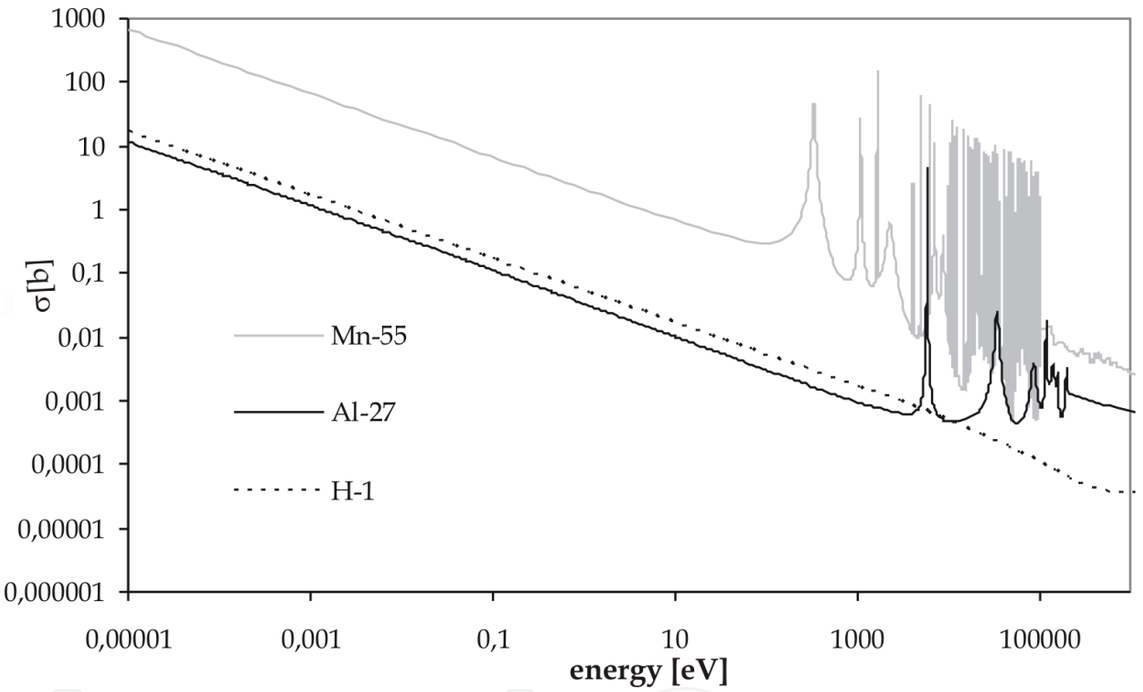

Fig. 2.2. The exemplary cross sections of simple capture reactions [12].

3. Method of identifications of radioisotopes

The base method of identification of the radioisotopes induced by therapeutic beams is a spectroscopy of gammas emitted by the originated unstable atomic nuclei.

In this paragraph the details of the method using the high-purity germanium detector is described (energy calibration of the detection system, the use of calibration sources and verification of the calibration during measurements of the spectra of gammas emitted by the radioisotopes etc.).

The complementary method of identification of the radioisotopes can be also based on the Monte Carlo computer simulation of physical processes and particle transportation inside the radiotherapy facility and in the walls, ceiling and floor of the room with a linac. The computation method based on the GEANT4 code will be described. The exemplary energy spectrum derived by the MC computer simulation will be presented and analysed.

3.1 The high-purity germanium detector

One of the base detectors that can be applied to identify radioisotopes originated inside the radiotherapy facility is the high-purity germanium detector applied for a field spectrometry. The detector is connected to a multichannel analyzer installed in a PC computer (usually in a laptop). The work of the detector is operated by the special software. All detection system is relatively small and it can be easy displaced. The high-purity germanium detectors are characterized by a good efficiency and resolution. It makes it possible to measure the photon energies from several dozen keV to several MeV. The low-energy limit depends on the thickness of the germanium crystal shield whereas the high-energy limit is connected with the size of the germanium crystal. The energy calibration (i.e. determination of energy for each channel of the multichannel analyzer) is usually performed with the use of set of commercial calibration sources. The view of the ORTEC high-purity germanium detector and its exemplary energy calibration curve is presented in Figure 3.1.

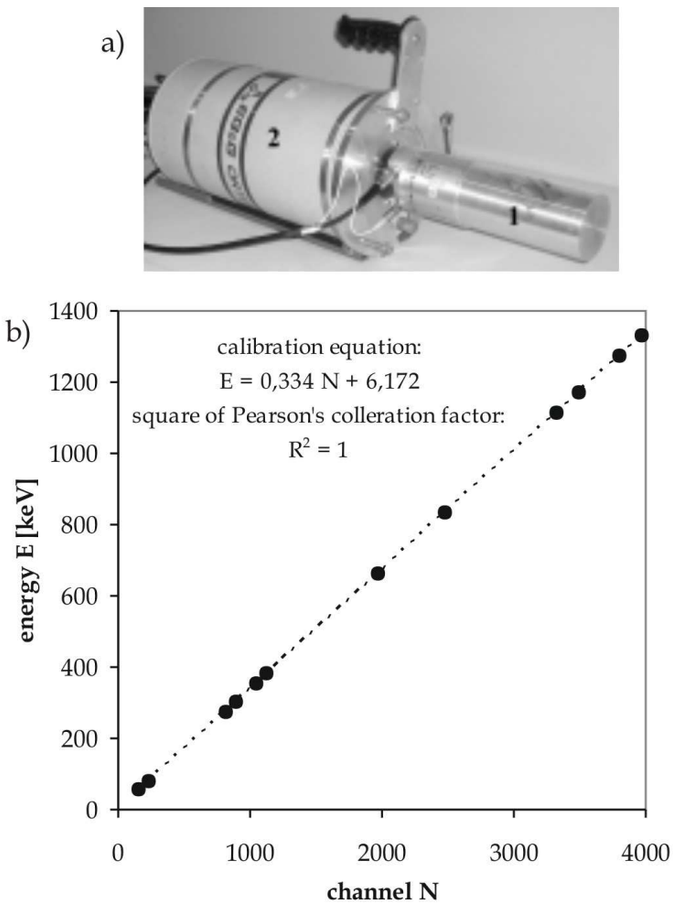

Fig. 3.1. The view of the high-purity germanium detector by ORTEC (1 – the aluminium shield of the germanium crystal, 2 - container with liquid nitrogen) a) and its energy calibration curve b). The following calibration sources were used to derive the calibration equation: ^{22}Na, ^{54}Mn, ^{60}Co, ^{74}Se, ^{133}Ba, ^{137}Cs, ^{241}Am. These seven sources give twelve points in the energy calibration curve (from 12 photons with various energies). The linear function is fitted to get the calibration equation. The square of the Pearson's correlation factor value - $R^2 = 1$ for the fit shows that the determined function is a good description of the obtained energy calibration curve.

The energy calibration can be checked in the measuring place. For this purpose, the block of the ^{115}In isotope is located inside the radiotherapy facility (for example on the therapeutic couch) in the field of neutrons from (γ,n) reactions occurring during the emission of the high-energy therapeutic X-ray beam. Indium is activated by thermal and resonance neutrons. The following neutron capture reaction takes place:

$$^{115}_{49}\mathrm{In} + ^{1}_{0}\mathrm{n} \rightarrow ^{116m}_{49}\mathrm{In(metastable)},$$

followed by radioactive decay:

$$^{116m}_{49}\mathrm{In} \xrightarrow[T_{1/2} = 54.41\,\mathrm{min}.]{} ^{0}_{-1}\mathrm{e} + ^{116}_{50}\mathrm{Sn}^{*} \rightarrow \gamma + ^{116}_{50}\mathrm{Sn}.$$

Six strong photopeaks from the deexcitation of the ^{116}Sn* state are used for the verification of the energy calibration of the detection system.
The details of the gamma spectroscopy were presented in many publications [see for example 1, 2].

3.2 Monte Carlo computer simulation by GEANT4

The spectra of gammas from the (e,e'n), (γ,n) and (n,γ) reactions can be derived by the Monte Carlo calculations realized with the use of the computer simulations.
The Monte Carlo calculation method seems to be the most comprehensive and potentially the most accurate method to derive such energy spectra. At present one of the dominant software that makes it possible to simulate the above mentioned reactions and others[1] occurring during emission of the high-energy therapeutic beams is the GEANT4 (GEometry ANd Tracking) code. This software has a form of C++ libraries prepared in CERN. GEANT4 is a good tool for modeling objects with complicated shape like a medical linac because it has plentiful predefined solid geometry types that can be combined via Boolean operations. This feature of the GEANT4 permits to make an accurate copy of the real object, which is the main condition to obtain the sensitive results. In Figure 3.2 the visualization of a fragment of a radiotherapy facility with a linac and a patient is presented. More information on GEANT4 is on the web side of the GEANT4 project [3] and in many publications [for example 4-6].

4. Radioisotopes originating from photonuclear and electronuclear reactions

The therapeutic gammas and electrons with appropriately high energy induce the nuclear reactions (γ,n) and (e,e'n) in which radioisotopes come into existence (see the explanation in Introduction). The therapeutic beam is collimated therefore the area of occurrence of these reactions is well determined except for the scattered gammas / electrons leaving the beam. However, the fluence of the scattered radiation outside the therapeutic beam is several

[1] The processes occurring during emission of the high-energy therapeutic electrons and X-rays: bremsstrahlung production, ionization, multiple scattering for electrons and positrons, positron annihilation, and additionally, photoelectric effect, Compton interaction, gamma conversion and Rayleigh scattering for photons, neutron capture, elastic and inelastic neutron scattering, decay process and some others of the lower significance, for example, the Auger effect ect.

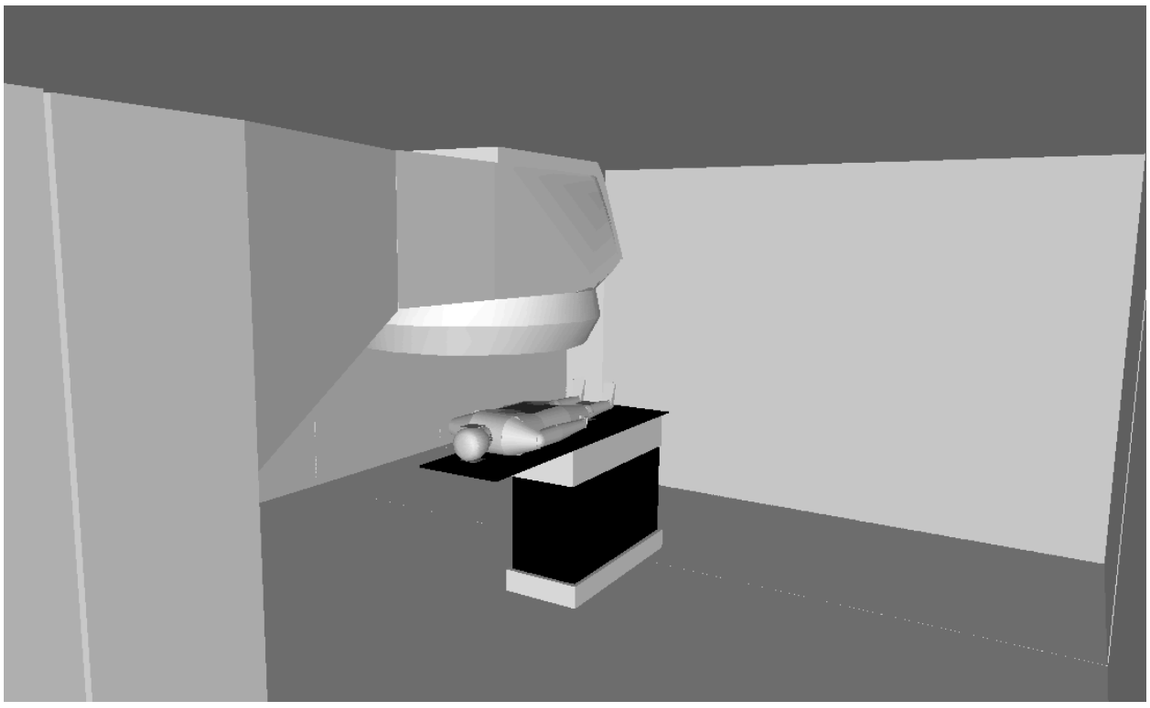

Fig. 3.2. The visualization of a fragment of the virtual model applied for the computer simulation of the high-energy X-ray irradiation of a patient. The simulation program was written with the use of the GEANT4 code. The picture was generated by the simulation program in a graphic mode of the VRML script.

orders of magnitude less than inside the beam. Thus, the photonuclear and electronuclear reactions occur mainly inside the therapeutic beam i.e. in the accelerator head and in air. Interactions between the therapeutic gammas and nuclei of ^{14}N and ^{16}O cause the photonuclear reactions giving two radioisotopes ^{13}N and ^{15}O:

$$\gamma + {}^{14}_{7}\mathrm{N}(99.6\%) \rightarrow {}^{1}_{0}\mathrm{n} + {}^{13}_{7}\mathrm{N}, \qquad \gamma + {}^{16}_{8}\mathrm{O}(99.8\%) \rightarrow {}^{1}_{0}\mathrm{n} + {}^{15}_{8}\mathrm{O}.$$

Abundance is given after the symbol of the nucleus in parenthesis. Such way of a reaction notation is used in this chapter. The nuclei: ^{13}N and ^{15}O disintegrate by β+ decay and electron capture (EC) into stable nuclei. The decay schemes of these two unstable nuclei are presented in Figure 4.1. The total cross section of the photonuclear reactions with ^{16}O is shown in Figure 4.2. The activation of the air was considered by many authors (see, for example [7]).

The contemporary commercial medical linacs have usually collimator system made of tungsten. However, target and flattening filter are made of various materials, dependently on the kind and energy of the therapeutic beam and on a manufacturer of an accelerator. In Figure 4.3 a spectrum measured under the head of one of the commercial medical accelerator with a gold target is presented. The peaks from gammas emitted by radioisotopes originating in the (γ,n), (e,e'n) and (n,γ)[2] reactions are marked.

[2] Radioisotopes originating from simple capture reactions are discussed in the next paragraph.

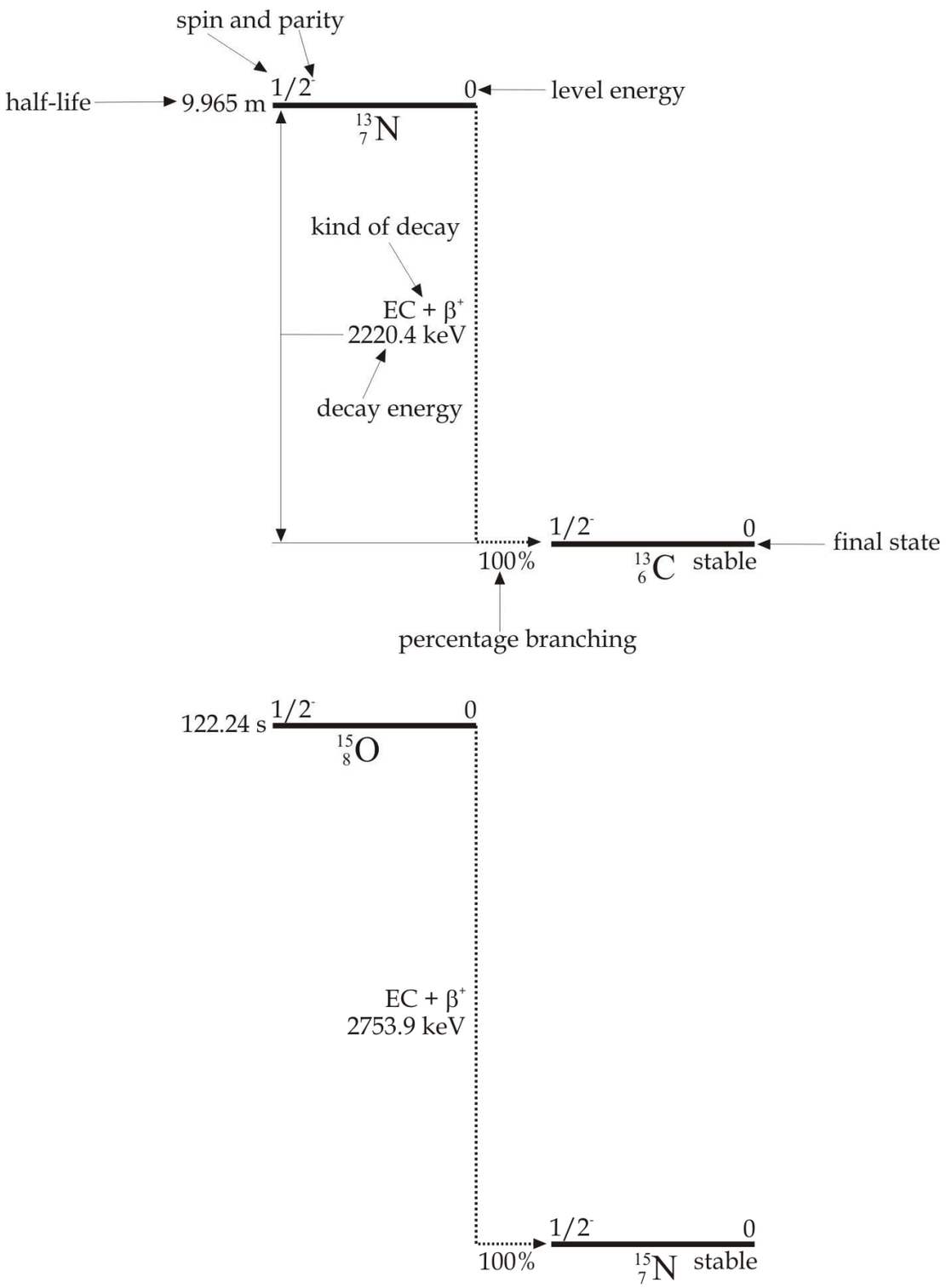

Fig. 4.1. Decay schemes of ^{13}N and ^{15}O – nuclei originating from photonuclear reactions induced by gammas of therapeutic X-ray beams. Explanation of the description of the formalism of all decay schemes presented in this chapter is given using the decay of ^{13}N.

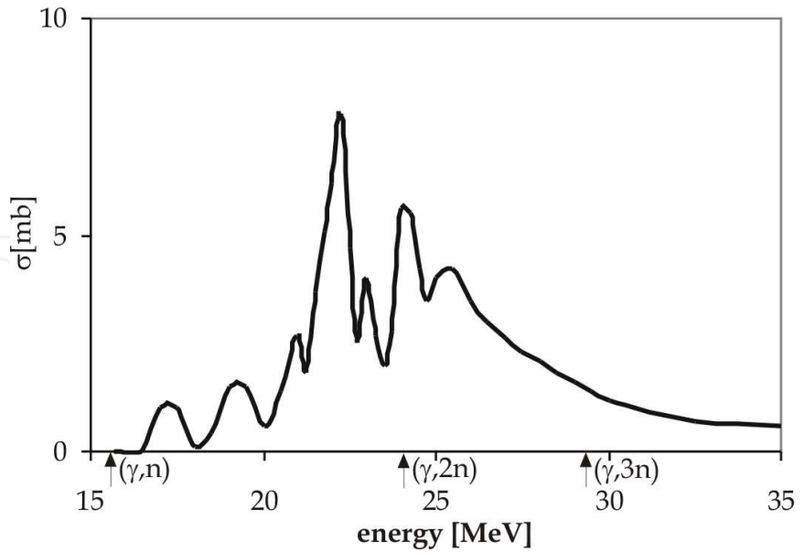

Fig. 4.2. The cross sections of the photonuclear reaction $^{16}O(\gamma,n)^{15}O$. The cross section for the analogous reaction with ^{14}N is presented in Figure 2.1. [12]

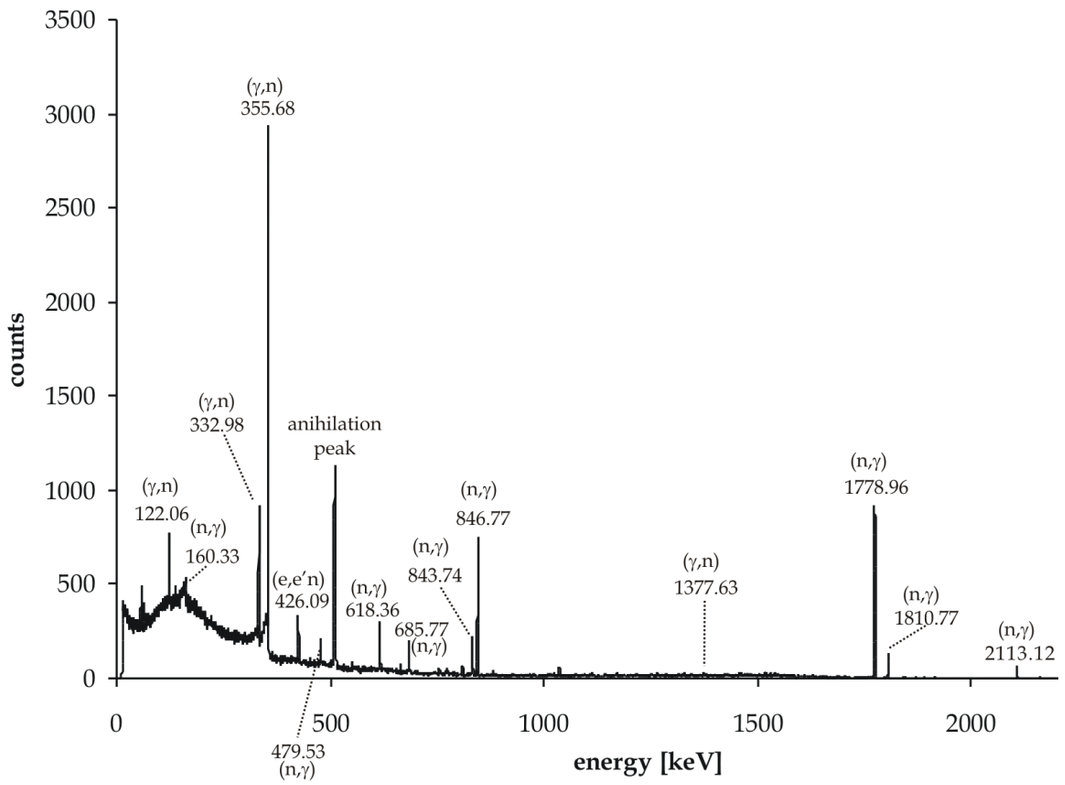

Fig. 4.3. The energy spectrum of gamma radiation measured under the head of a commercial medical linac with the gold target. The peaks come from decays of radioisotopes originated from photonuclear, electronuclear and simple capture reactions (see notation near the peaks).

The annihilation peak[3] visible in Figure 4.3 comes from β⁺-emitters. Moreover, gamma with energies over 1022 keV can create a pair of electron-positron in the nucleus field. The created positron reaching thermal energy can undergo annihilation. Two radioisotopes: ^{196}Au and ^{57}Ni came into being as a result of the photonuclear and electronuclear reactions. The radioisotope ^{196}Au can originate from the following reactions:

$$\gamma + {}^{197}_{79}\mathrm{Au}(100\%) \rightarrow {}^{1}_{0}\mathrm{n} + {}^{196}_{79}\mathrm{Au}, \qquad {}^{0}_{-1}\mathrm{e} + {}^{197}_{79}\mathrm{Au} \rightarrow {}^{0}_{-1}\mathrm{e}' + {}^{1}_{0}\mathrm{n} + {}^{196}_{79}\mathrm{Au}.$$

The maximum value of the cross section of the reaction ^{197}Au(γ,n)^{196}Au is about 580 mb and it corresponds to neutron energy of about 14 MeV [11]. Gold is characterized by the relatively high cross section for the neutron capture reaction - ^{197}Au(n,γ)^{198}Au (i.e. the total thermal neutron capture cross section of 96 barns and the resonance activation integral of 1558 barns [8, 9]). However, the gammas (411.8 keV) from the decays of nuclei of ^{198}Au are absent in the presented spectrum measured under the accelerator head since the fast neutrons originate in the target and they leave it before slowing down to the thermal and resonance energies. The production of another radioisotope ^{195}Au (EC + β⁺, $T_{1/2}$ = 186.1 d, decay energy of 226.8 keV, energy of emitted gammas of 98.9 keV [13]) is possible in the (γ,2n) reaction. However, the energy threshold of this reaction is 15 MeV [11].
The photonuclear reaction from which the radioisotope - ^{57}Ni originates, can be expressed as

$$\gamma + {}^{58}_{28}\mathrm{Ni}(68.1\%) \rightarrow {}^{1}_{0}\mathrm{n} + {}^{57}_{28}\mathrm{Ni}.$$

The maximum value of the cross section of this reaction is about 30 mb and it corresponds to gamma energy of about 17 MeV [11]. Nickel is the main component of stainless steel used in a construction of medical accelerators. The decay schemes of nuclei of ^{196}Au and ^{57}Ni are presented in Figures 4.4 and 4.5, respectively.

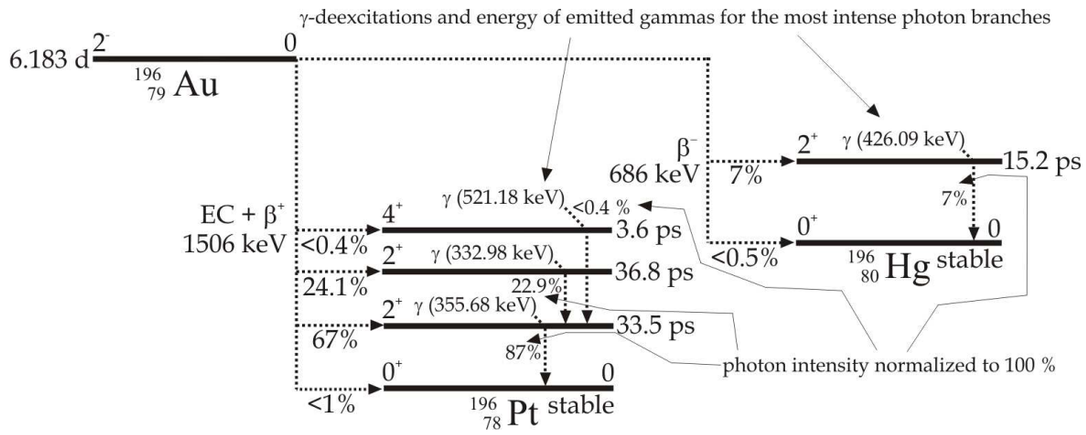

Fig. 4.4. Decay scheme of the ^{196}Au nucleus originating from photonuclear reaction induced by gammas of therapeutic X-ray beam in the target of medical linac. The γ-deexcitation notation used for the excited states of ^{196}Pt and ^{196}Hg is valid in this entire chapter. The peaks from gammas with energies of 355.68 keV, 332.98 keV and 426.09 keV are visible in the spectrum measured under the accelerator head (see Figure 4.3).

[3] The annihilation peak is created by gammas with energy of 511 keV corresponding to the rest mass of an electron or a positron.

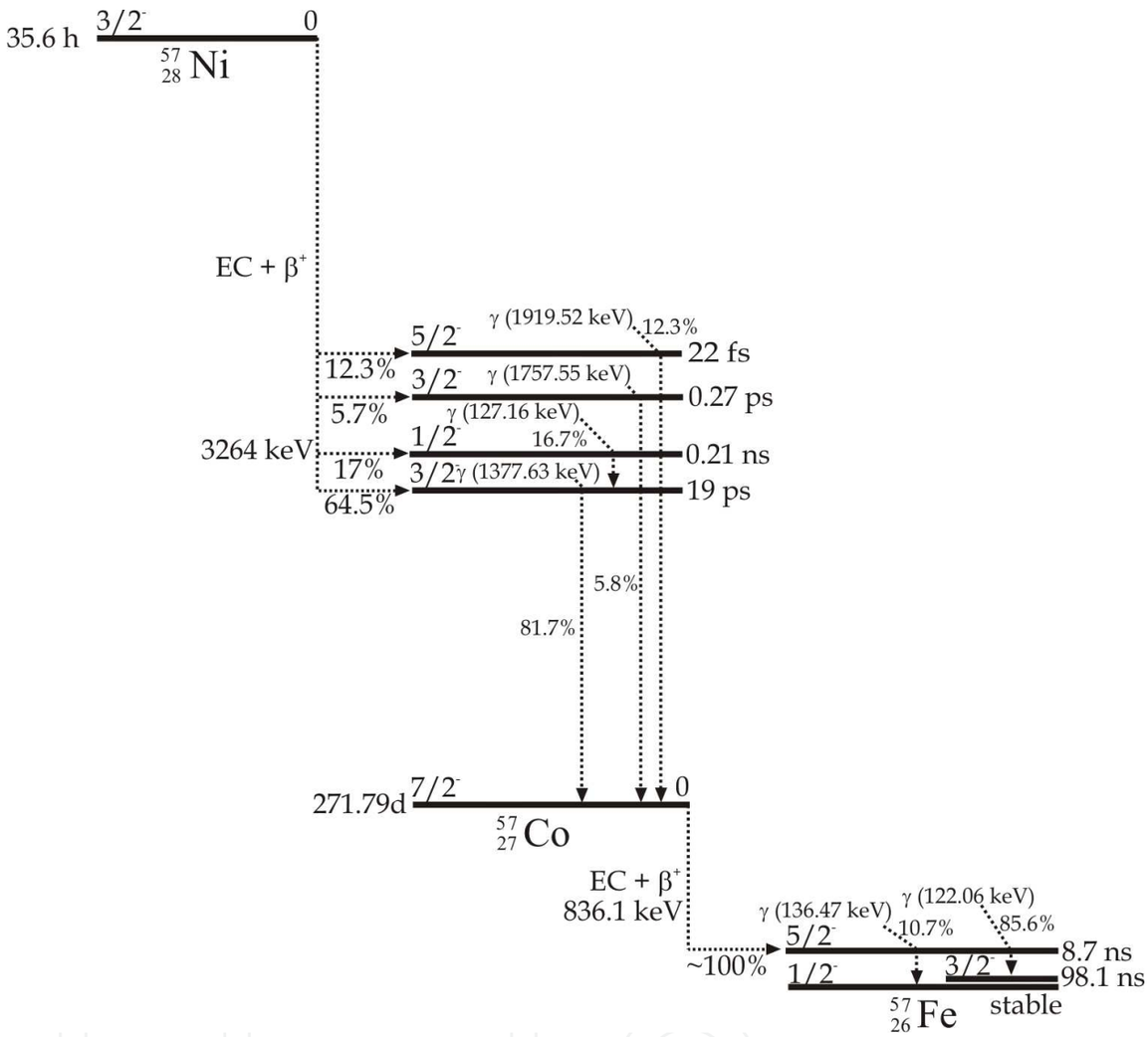

Fig. 4.5. Decay schemes of the ^{57}Ni nucleus and its daughter nucleus - ^{57}Co. The peaks at 1377.55 keV and at 122.06 keV from gammas of two most intense photon branch are visible in the spectrum measured under the accelerator head (see Figure 4.3).

Massive accessories of medical linacs, like wedges, electron applicators etc., are often located inside a high-energy therapeutic beam and they are activated in the (γ,n) and (e,e'n) reactions. The linac accessories can also be activated outside the therapeutic beam, by neutrons from the photonuclear and electronuclear reactions. Massive accessory of linacs are designed to collimate the beam or to change the beam profile etc. They are often made of lead, tungsten and stainless steel. The exemplary energy spectrum of gammas emitted by radioisotopes induced in the typical medical accelerator accessory is presented in Figure 4.6.

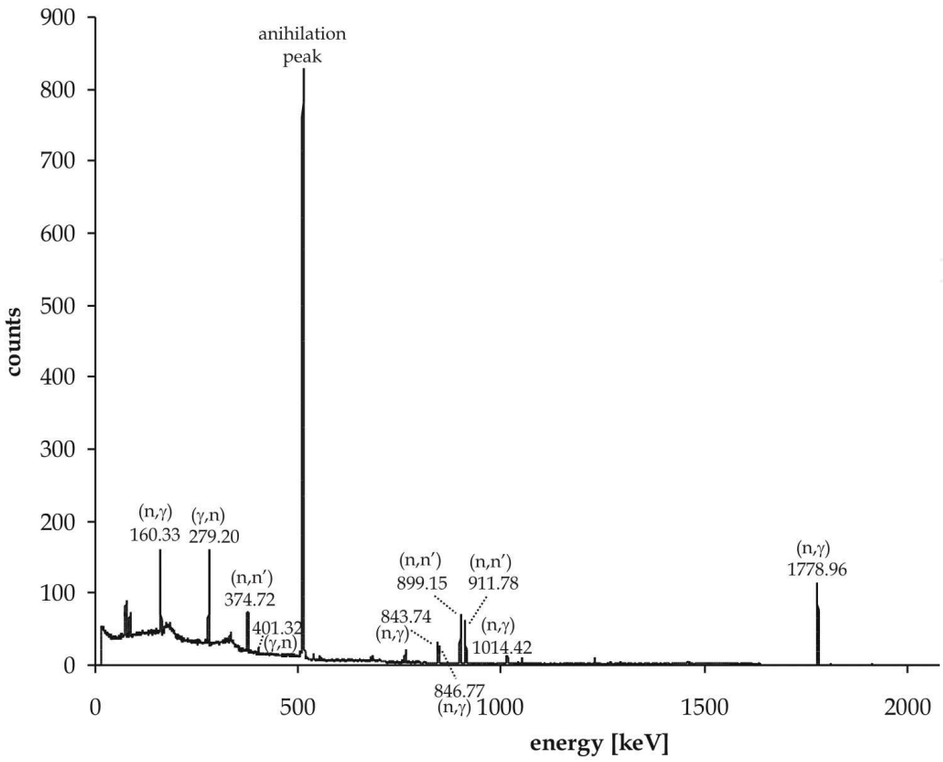

Fig. 4.6. The typical energy spectrum of gammas emitted by a medical linac accessory. The notation near the peaks is as in Figure 4.3.

The peaks at 279.20 keV and at 401.32 keV are a result of the following photonuclear reaction:

$$\gamma + {}^{204}_{82}\mathrm{Pb}(1.4\%) \rightarrow {}^{1}_{0}\mathrm{n} + {}^{203}_{82}\mathrm{Pb},$$

followed by electron capture and β^+ decay giving the excited state of ^{203}Tl* (Figure 4.7).

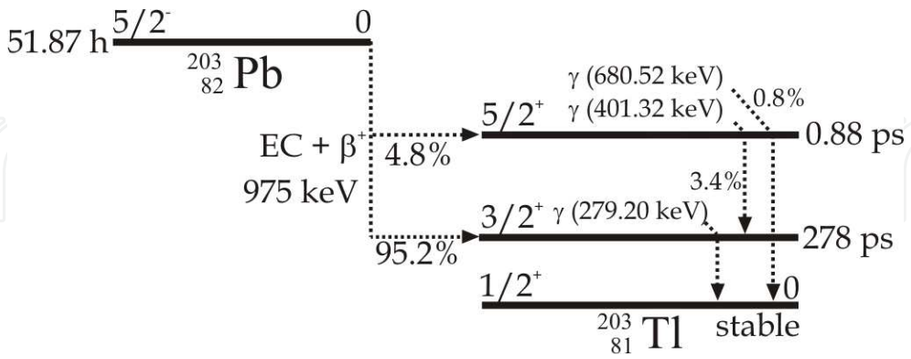

Fig. 4.7. Decay scheme of the ^{203}Pb nucleus. The gammas with energies of 279.20 keV and of 401.32 keV, from the deexcitation of ^{203}Tl* give the peaks visible in the spectrum of gammas emitted by a medical linac accessory (see Figure 4.6).

There are four natural stable isotopes of lead: ^{204}Pb (abundance of 1.5 %), ^{206}Pb (24.1 %), ^{207}Pb (22.1 %) and ^{208}Pb (52.3 %) which can give three radioisotopes: ^{203}Pb (mentioned above), ^{205}Pb and ^{209}Pb (Figure 4.8). First two of them are a result of photonuclear reactions whereas

third originates from neutron capture reaction (see next paragraph). Decays of ^{205}Pb and ^{209}Pb nuclei occur without emission of gammas. Thus, identification of these radioisotopes cannot be based on the gamma spectroscopy. However, appearance of the radioisotope ^{203}Pb decaying with gamma emission, originating from the isotope ^{204}Pb with abundance smallest of all natural lead isotopes indicates to appearance of the radioisotopes: ^{205}Pb and ^{209}Pb, because the (γ,n) cross sections are of the similar value for all isotopes of lead (the total photoneutron cross section for natural lead ~3047 mb [11]), and the total thermal neutron cross section for ^{208}Pb(n,γ)^{209}Pb is relatively high to be 0.49 b[12]. Additionally, ^{202}Pb can originate as a result of (γ,2n) reaction for the beam with a nominal potential of 18 MV or higher (photon energy threshold of this reaction ~ 15 MeV).

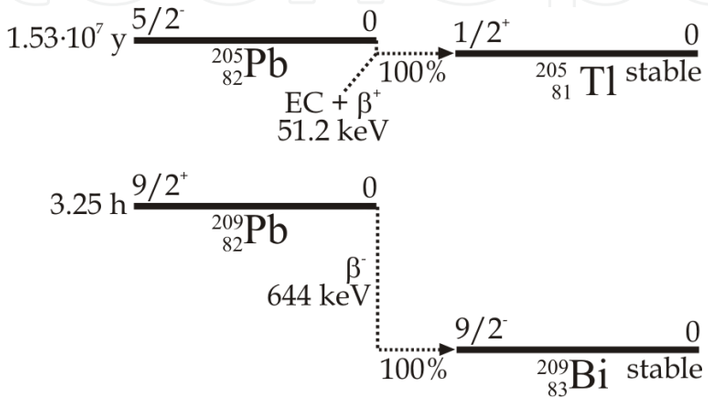

Fig. 4.8. Decay schemes of the ^{205}Pb and ^{209}Pb nuclei.

In general, the analogical considerations can be conducted for other radioisotopes. In the presented way the appearance of the radioisotope: ^{59}Ni and ^{63}Ni can be evidenced. The first radioisotope comes into being from ^{60}Ni (26.2 %) in the photonuclear reaction and the second from ^{62}Ni (3.6 %) in the neutron capture reaction. The radioisotope ^{63}Ni can also originate from the photonuclear reaction with ^{64}Ni. The neutron capture reaction with ^{64}Ni can give radioisotope ^{65}Ni but it is not considered because of a small abundance of ^{64}Ni (less than 1 %). Decay schemes of ^{59}Ni and ^{63}Ni nuclei are presented in Figure 4.9.

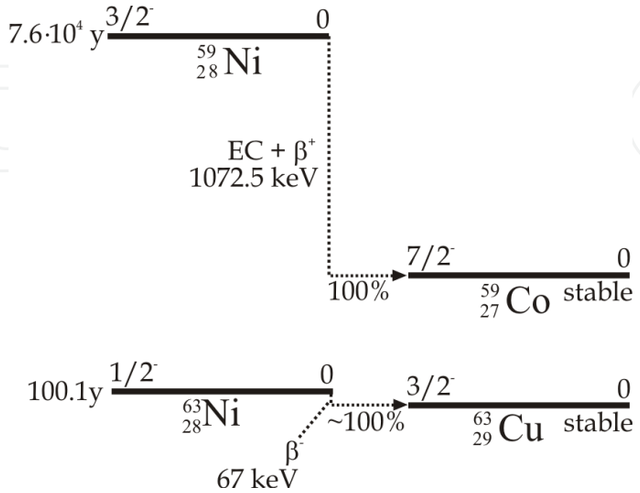

Fig. 4.9. Decay schemes of the ^{59}Ni and ^{63}Ni nuclei.

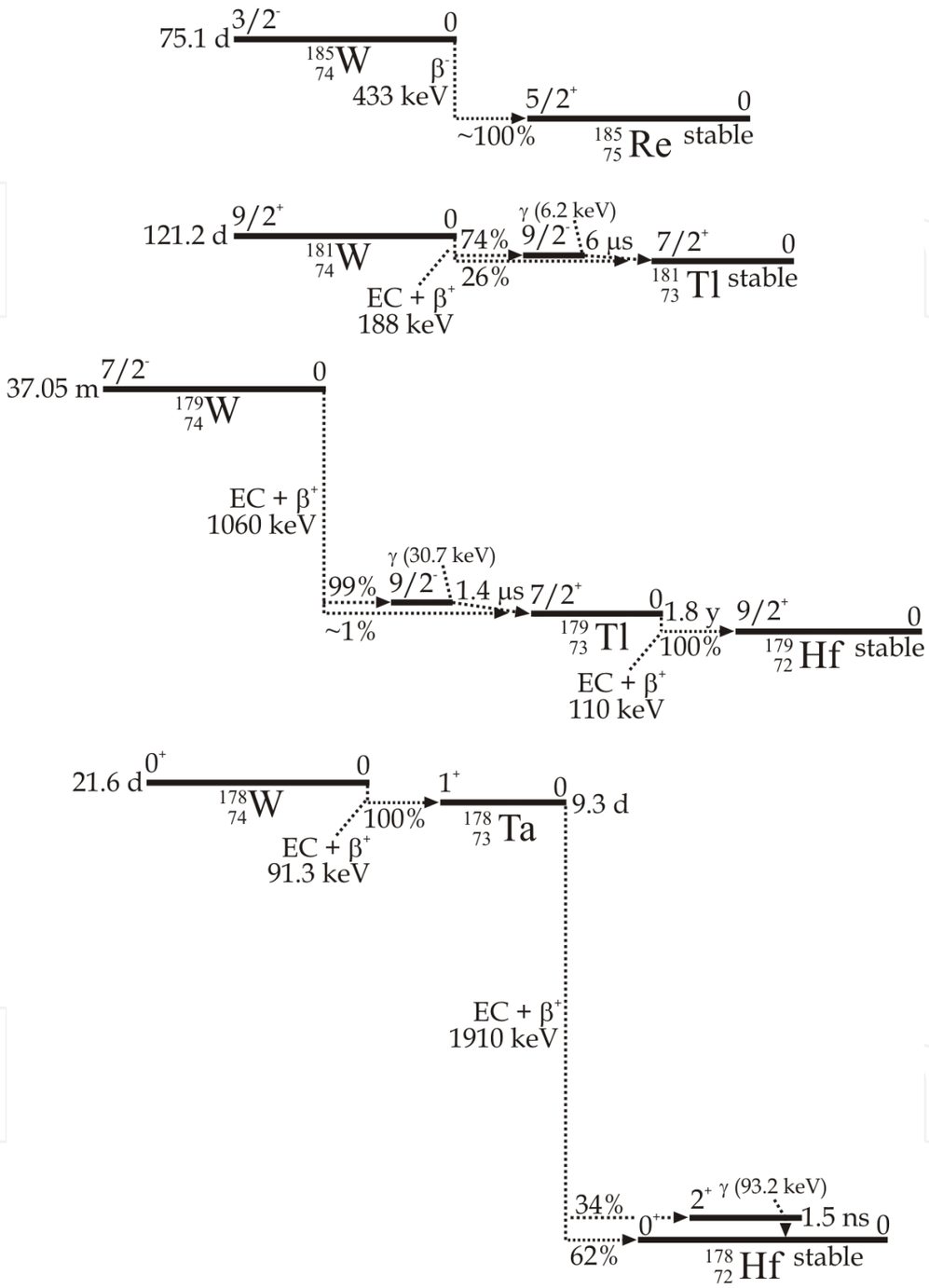

Fig. 4.10. Decay schemes of the ^{178}W, ^{179}W, ^{181}W and ^{185}W nuclei originating from photonuclear or electronuclear reactions. The gammas from the decays of these tungsten radioisotopes are difficult to identify by the gamma spectroscopy because of relatively low energy. The peaks from these gammas are not visible in the spectrum measured under the accelerator head contrary to the gammas from the decay of ^{187}W (see Figure 4.3). Low-energy peaks from decays of nuclei can be concealed among peaks from scattered radiation.

As it was mentioned above, the collimator system of the contemporary medical linacs is usually made of tungsten. Thus, constructions of the linac heads are characterized by a great amount of tungsten. There are five natural stable isotopes of tungsten: ^{180}W (0.1 %), ^{182}W (26.3 %), ^{183}W (14.3 %), ^{184}W (30.7 %) and ^{186}W (28.6 %). Three of them (i.e. ^{180}W, ^{182}W and ^{186}W) can be changed into radioisotopes in photonuclear and electronuclear reactions. Two of them (i.e. ^{183}W and ^{184}W) change into stable nuclei in the mentioned reactions. The radioisotopes: ^{179}W, ^{181}W and ^{185}W originate from the nuclei of ^{180}W, ^{182}W and ^{186}W, respectively, after separation of one neutron. The radionuclide ^{178}W comes into existence after separation of two neutrons from the nucleus of ^{180}W. The energy threshold for the reaction – ^{180}W(γ,2n)^{178}W is about 15 MeV. The total photoneutron cross section for natural tungsten is 2854 mb [11]. Decay schemes of the tungsten radioisotopes originating from photonuclear or electronuclear reactions are presented in Figure 4.10.

5. Radioisotopes originating from simple capture reactions

The neutrons from the photonuclear and electronuclear reactions induced by high-energy electron and X-ray therapeutic beams can interact with nuclei of atoms of matters inside the radiotherapy facility. The neutrons interact mainly in simple capture reactions. The (n,γ) reaction cross sections are particularly high in the range of thermal and resonance energies (see paragraph 2.3). Inelastic scattering of neutrons is less possible. Radioisotopes decaying by emission of β^- radiation mainly come into existence as a result of the simple capture reactions whereas radioisotopes originating from photonuclear and electronuclear reactions disintegrate by electron capture or β^+ decay. It is connected by the fact that simple capture reactions cause the increase of a number of neutrons in a nucleus. A nucleus becomes neutron-rich and it attains more stable configuration by a change of a neutron into a proton. Analogically, photonuclear and electronuclear reactions cause the decrease of a number of neutrons. A nucleus becomes proton-rich and it attains "curve of stability" by a change of a proton into a neutron.

The simple capture reactions can occur in the whole area of the treatment room, because the field of thermal and resonance neutrons is approximately uniform around the working linac [10]. Thus, radioisotopes can originate in all objects inside the treatment room, regardless of their distance from the therapeutic beam.

The radioisotopes: ^{181}W and ^{185}W mentioned in the previous paragraph can also originate from simple capture reactions even outside the therapeutic beam. The radioisotope ^{187}W comes into existence only by the capture of neutron:

$$^{1}_{0}\mathrm{n} + {}^{186}_{74}\mathrm{W}(28.6\%) \rightarrow \gamma + {}^{187}_{74}\mathrm{W}.$$

This reaction is characterized by the neutron thermal cross section of 37.9 b [12] greatest of all natural tungsten isotopes and by the relatively large resonance activation integral of 355 barns [14]. Decay of the originated radioisotope - ^{187}W is connected with emission of gammas (Figure 5.1). Thus, this radioisotope can be identified by the gamma spectroscopy (see Figure 4.3). The maximum range of electrons from the β^- decay of ^{187}W is $R_{m,air}$ = 429 cm in air and $R_{m,bt}$ = 0.6 cm in a biological tissue[4].

[4] The maximum ranges of electrons from the β^- decay in air (denoted as $R_{m,air}$) and in a biological tissue (denoted as $R_{m,bt}$) were calculated on the base of equivalent values of exposure constant given by Gostkowska in [15]. The air density of 0.0013 g/cm^3 and the biological tissue density of 1 g/cm^3 were taken for the calculations of the electron ranges.

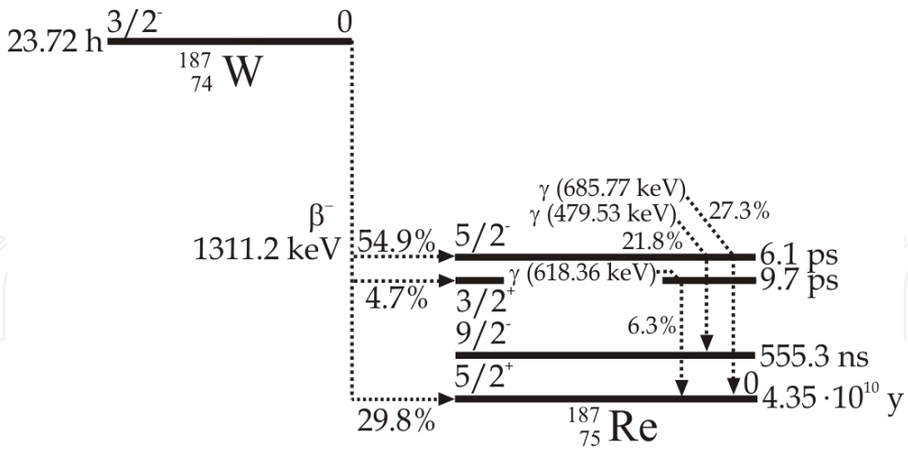

Fig. 5.1. Decay scheme of the ^{187}W nucleus. The gammas with energies of 479.53 keV, 618.36 keV and of 685.77 keV, from the deexcitation of the state ^{203}Re* give the peaks visible in the spectrum measured under the accelerator head (see Figure 4.3). This scheme includes the most photon branches of the decay.

In the spectrum measured under the medical linac head (Figure 4.3) as well as in the spectrum of gammas emitted by a medical linac accessory (Figure 4.6) the peaks from the decay of ^{56}Mn (Figure 5.2) are visible. Manganese - ^{55}Mn in the stable state (the only natural isotope of manganese), like Nickel, is one of the fundamental components of stainless steel used in a construction of medical accelerators. This isotope is easily activated by neutrons because it has a large cross section for the neutron capture i.e. the thermal neutron capture cross section is 13.2 b, and the resonance activation integral is 15.7 b (the high resonance peak occurs at 337 eV) [12]. The simple capture reaction giving the ^{56}Mn radioisotope can be expressed as follow:

$$ {}^{1}_{0}\mathrm{n} + {}^{55}_{25}\mathrm{Mn}(100\%) \rightarrow \gamma + {}^{56}_{25}\mathrm{Mn}. $$

The ^{56}Mn radioisotope disintegrates by emission of β$^-$ radiation. The maximum range of emitted electrons is $R_{m,air}$ = 1256 cm in air and $R_{m,bt}$ = 1.6 cm in a biological tissue.
The peak at 1778.96 keV, visible in the spectra presented in Figures 4.3 and 4.6, comes from the decay of the ^{28}Al radioisotope originating from the following reaction:

$$ {}^{1}_{0}\mathrm{n} + {}^{27}_{13}\mathrm{Al}(100\%) \rightarrow \gamma + {}^{28}_{13}\mathrm{Al}. $$

The cross section for this reaction is 0.231 b at the thermal energy and it decreases for higher energy and one greater resonance of 4.685 b occurs at 5904 keV [12]. The only natural isotope of aluminum – ^{27}Al is a material applied in the radiation absorbers located inside the primary collimator under the target and also in the construction of other components of a linac head, for example in dose chambers and in wedge trays. The decay scheme of the ^{28}Al radioisotope is presented in Figure 5.3. Decay of the ^{28}Al nucleus is connected not only with emission of gammas but also with emission of β$^-$ radiation. The maximum range of electron from this decay is close to that from the decay of the ^{56}Mn nuclei i.e. $R_{m,air}$ = 1265 cm, $R_{m,bt}$ = 1.6 cm.

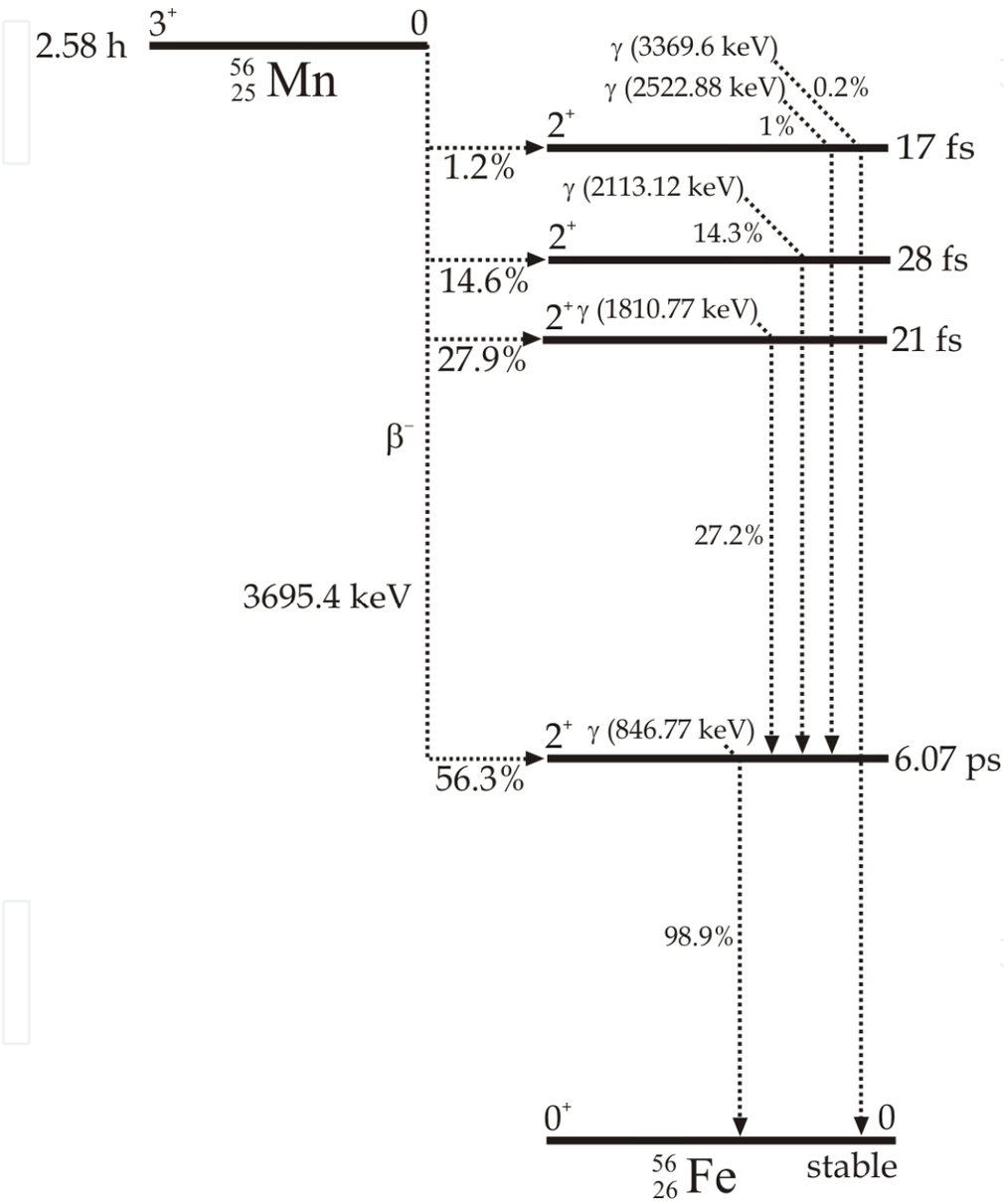

Fig. 5.2. Decay scheme of the ^{56}Mn nucleus.

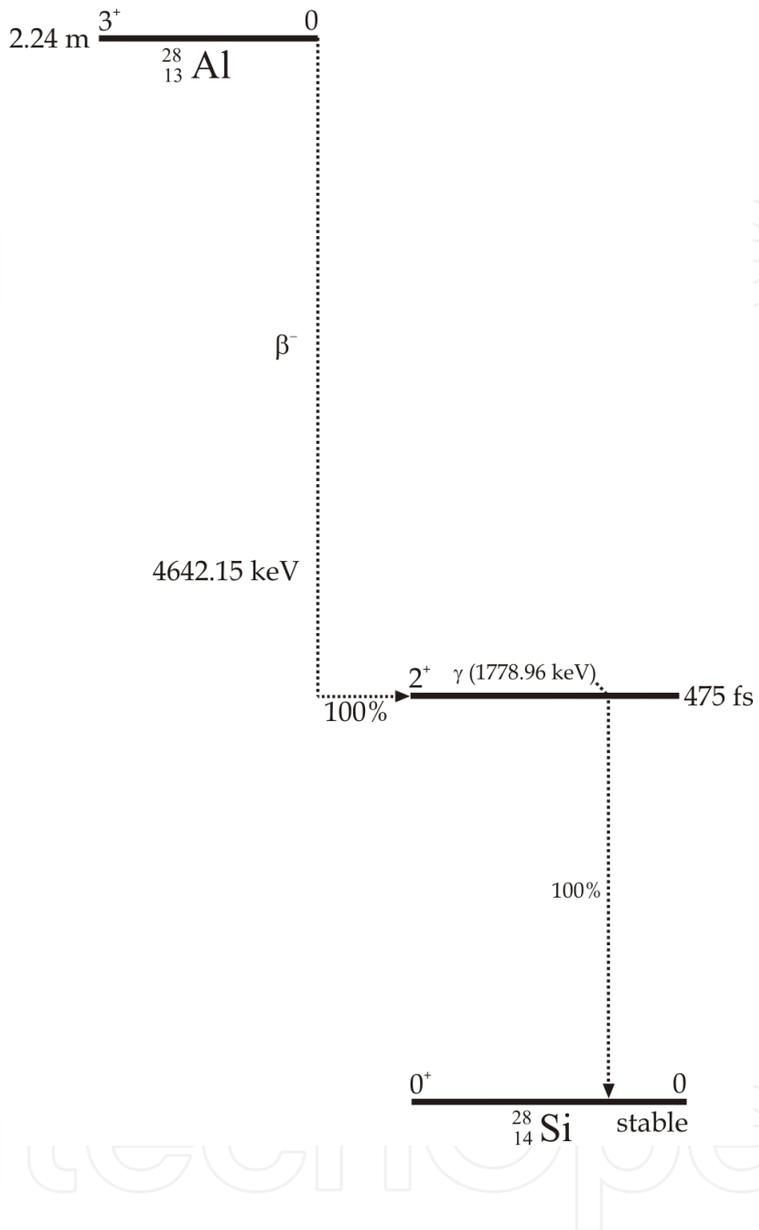

Fig. 5.3. Decay scheme of the ^{28}Al nucleus.

One of the strongest peaks in the spectrum of gammas emitted by the accessory of a medical linac (Figure 4.6) is that at 160.33 keV. It comes from the disintegration of the ^{123}Sn nuclei originated from the following reaction:

$$^{1}_{0}\mathrm{n} + ^{122}_{50}\mathrm{Sn}(4.7\%) \rightarrow \gamma + ^{123}_{50}\mathrm{Sn}.$$

The decay scheme of the ^{123}Sn nucleus is presented in Figure 5.4. Electrons from the β- decay of this radioisotope have $R_{m,air}$ = 400 cm and $R_{m,bt}$ = 0.5 cm.

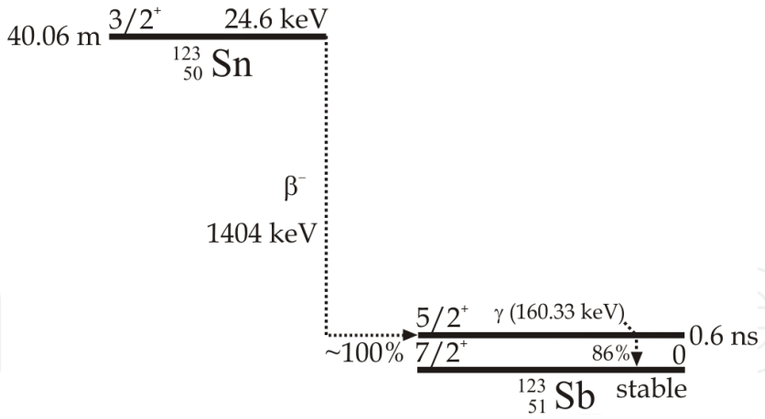

Fig. 5.4. Decay scheme of the ^{123}Sn nucleus.

The neutrons from (γ,n) reactions taking place in the components of the medical accelerator head have a broad energy spectrum inside the radiotherapy facility (see [17, 18]). Fast neutrons undergo elastic and inelastic scatterings. The neutron inelastic interaction provides nucleons of a nucleus with energy. The radioisotopes and nuclei in metastable states can be induced as a result of such interactions. In the spectrum of gammas emitted by the linac accessory the ^{204m}Pb metastable state was identified. It comes from inelastic interactions between neutrons and nuclei of ^{204}Pb:

$$ {}^{1}_{0}\mathrm{n} + {}^{204}_{82}\mathrm{Pb}(1.4\%) \rightarrow {}^{1}_{0}\mathrm{n}' + {}^{204m}_{82}\mathrm{Pb}. $$

The scheme of disintegration of the metastable ^{204m}Pb state is presented in Figure 5.5.

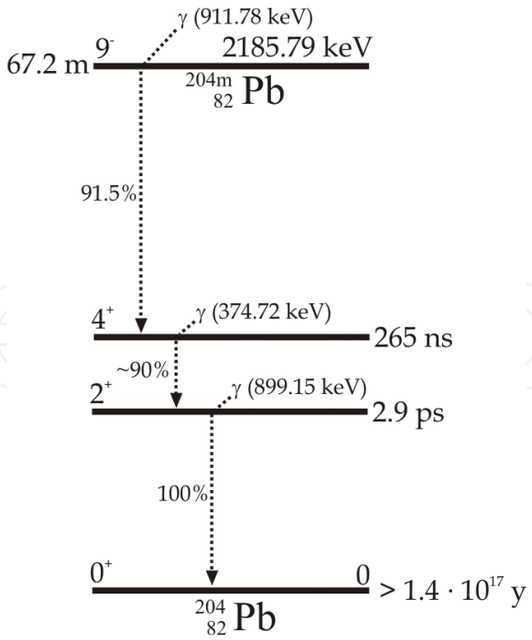

Fig. 5.5. Decay scheme of the ^{124m}Pb state. The peaks at 374.72 keV, 899.15 keV and of 911.78 keV are visible in the spectrum of gammas emitted by the accessory of a medical linac (Figure 4.6).

In the previous paragraph the ^{209}Pb radioisotope was mentioned to be a result of the simple capture reaction. The ^{209}Pb nuclei disintegrate by β- decay (Figure 4.8). The maximum range of electrons from this β- decay is $R_{m,air}$ = 173 cm in air and $R_{m,bt}$ = 0.2 cm in a biological tissue. Contribution of this radioisotope to a β- radiation level around the linac head can be significant because it originates from ^{208}Pb - the isotope with the abundance greatest of all natural lead isotopes. Moreover, lead is often used for construction of big components of the accelerator head like radiation shields, and also for individual shields[5] for patients.
Gold is often used in the construction of medical linacs, for example, connectors of wires are often made of Au (see also considerations for Figure 4.4). Gold has a relatively high cross section of the slowed down neutron simple capture reaction - ^{197}Au(n,γ)^{198}Au. Therefore the radioisotope ^{198}Au can easy come into existence in whole accelerator room. The energy spectrum of the gamma radiation from disintegration of the ^{198}Au nuclei, measured after a neutron activation of gold is presented in Figure 5.6. Decay scheme of the ^{198}Au nucleus is shown in Figure 5.7.

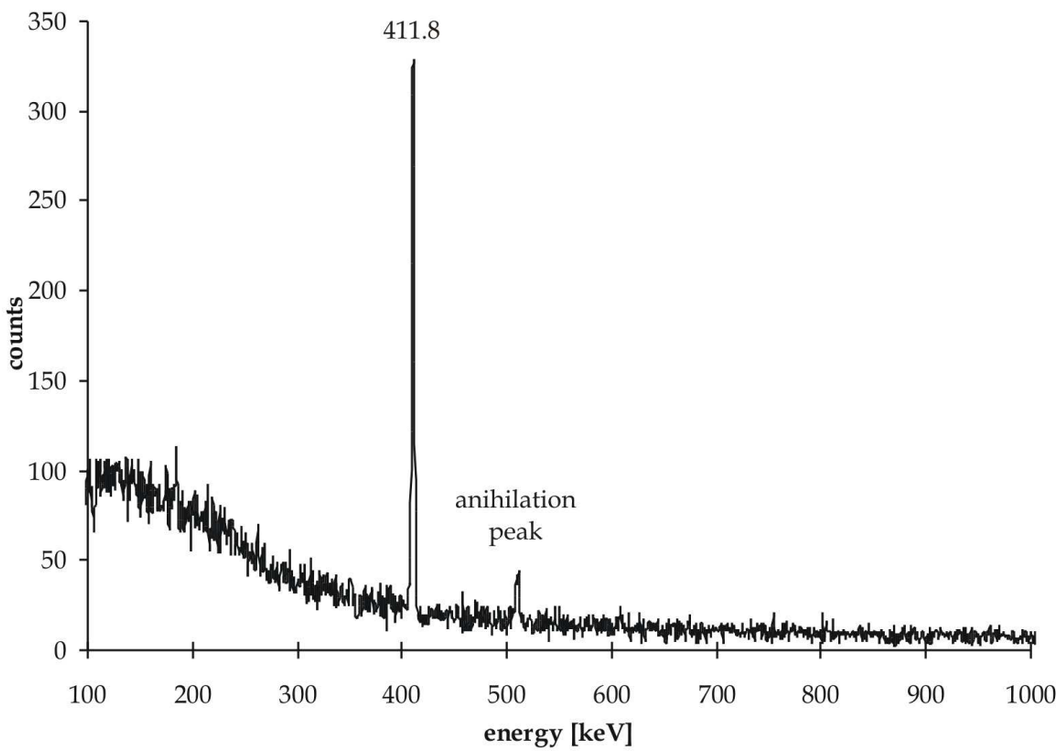

Fig. 5.6. The spectrum of gammas emitted by the ^{198}Au radioisotope. The spectrum was measured after the end of the neutron activation of gold.

[5] The individual shields for patients are often made of wood's melt which includes over 60 % of lead.

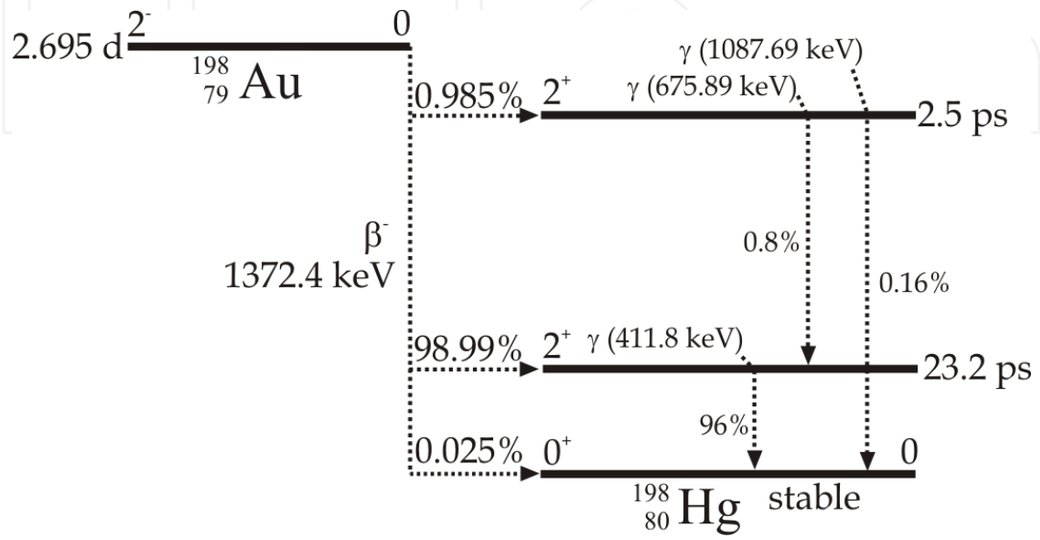

Fig. 5.7. Decay scheme of the ^{198}Au nucleus.

The simple capture reactions can be identified by binding energy of a neutron. Photons from these reactions are emitted by a nucleus immediately after capture of a neutron. However, in this case there appears the experimental difficulty connected with the fact that the gamma energy spectrum has to be measured during the occurrence of simple capture reactions. Thus, measuring apparatus has to be in the neutron field during such measurement and the neutrons interact with a detector and electronics of the detection system. The radioisotopes can be induced in materials of the detection system as a result of theses interactions. It can give an additional significant contribution to the measured energy spectrum and it can even disturb a measurement in many cases. The exemplary energy spectrum of gammas from simple capture reactions: ^{206}Pb(n,γ)^{207}Pb and ^{207}Pb(n,γ)^{208}Pb, induced mainly by thermal and resonance neutrons[6] is presented in Figure 5.8. To avoid the above described problems, the spectrum was obtained with the use of the Monte Carlo calculations.

[6] The reaction ^{206}Pb(n, γ)^{207}Pb has the high resonance of 309 b at 3.36 keV whereas the reaction ^{207}Pb(n, γ)^{208}Pb has the high resonance of 267 b at 3.06 keV [14].

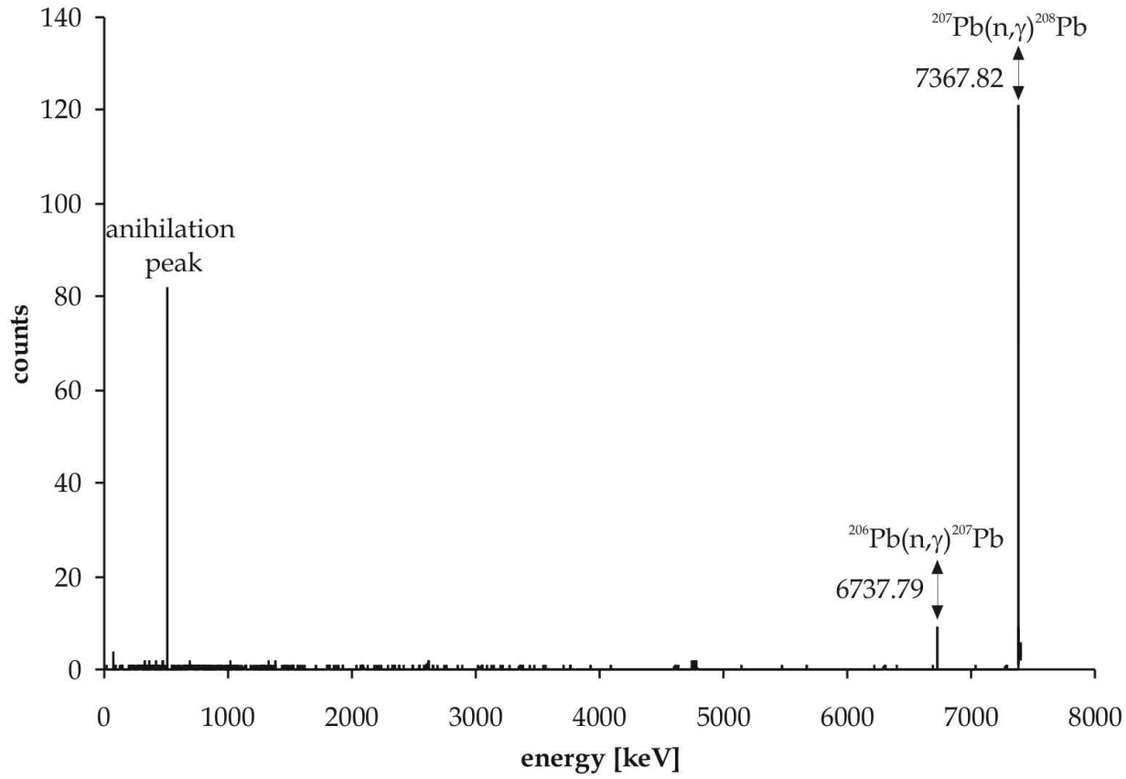

Fig. 5.8. The spectrum of gammas (6737.79 keV and 7367.82 keV) originating from the simple captures reactions: ^{206}Pb(n,γ)^{207}Pb and ^{207}Pb(n,γ)^{208}Pb. The spectrum was calculated by the Monte Carlo method, using computer simulations based on the GEANT4 code.

6. Conclusions

The radioactivity induced inside the radiotherapy facility is a consequence of the photonuclear and electronuclear reactions as well as the neutron reactions. The following radioisotopes originate as a result of the (γ,n), (γ,2n) and (e,e'n) reactions: ^{13}N, ^{15}O, ^{57}Co, ^{57}Ni, ^{59}Ni, ^{178}W, ^{179}W, ^{181}W, ^{185}W, ^{196}Au, ^{202}Pb, ^{203}Pb and ^{205}Pb. The (n,γ) and (n,n') reactions give the radioisotopes of ^{28}Al, ^{56}Mn, ^{63}Ni, ^{123}Sn, ^{187}W, ^{198}Au, ^{205}Pb, ^{209}Pb and the metastable state of lead - ^{204m}Pb. Most of the activated materials are the building materials of the head of the commercial accelerators used in the teleradiotherapy treatment.

The radioactivity inside the radiotherapy facility can be accumulated because in the majority the half-lives of the induced radioisotopes are between tens of minutes to several days. Moreover, the level of this induced radiation is connected with the kind of the therapeutic beams and the nominal potential of the beams [see 19], because the cross sections of the (γ,n) and (e,e'n) reactions depend on energy of gammas and electrons.

The good solution of the problem of the air activation is an uninterrupted ventilation of the radiotherapy facility, which makes it possible to reduce amount of the radioisotopes of ^{13}N and ^{15}O. The longer lasting emission of the high-energy X-ray beams should be avoided if it possible.

The knowledge of the neutron reactions taking place inside the radiotherapy facility is of great worth for designers of accelerators because elements with the large cross section of the neutron capture reactions can be eliminated from the accelerator construction. The information on the radioisotopes induced inside the radiotherapy treatment can be used in the radiological protection of the staff operating the medical accelerators.

7. References

[1] International Commission on Radiation Units and Measurements, Gamma-Ray Spectrometry in the Environment, „ICRU Report 53", Maryland, December 1994.
[2] International Electrotechnical Commission, In-situ photon spectrometry using a germanium detector for measuring discrete radionuclides in the environment, „IEC 209 FDIS", May 1992.
[3] http://geant4.web.cern.ch
[4] Konefał, A., 2006, Monte Carlo simulations with the use of the GEANT4 code. „Postępy Fizyki", 57(6): 242–251 (in Polish).
[5] Carrier J.-F., Archambault L., Beaulieu L., 2004, Validation of GEANT4, an object-oriented Monte Carlo Toolkit, for simulation in medical physics, „Med. Phys. ", 31, 484-492.
[6] Konefał, A., Szaflik P., Zipper, W., 2010, Influence of the energy spectrum and the spatial spread of the proton beams used in the eye tumor treatment on the depth-dose characteristics. „Nukleonika", 55(3): 313–316.
[7] Evdokimoff, V., Willins, J., Richter, H., 2002, Induced radioactive potential for a medical accelerator., „Health Physics", Operational Radiation Safety, 83, Sup.5:S68–S70.
[8] Price, W.J. Nuclear Radiation Detection. (USA: McGraw-Hill Book Company) (1964).
[9] Beckurc, K. and Wirtc, K. (eds), 1968, Niejtronnaja fizika. „Moscow: Atomizdat".
[10] Konefał, A., Polaczek-Grelik, K., Orlef, A., Maniakowski, Z., Zipper, W., 2006, Background neutron radiation in the vicinity of Varian Clinac-2300 medical accelerator working in the 20 MV mode., „Polish Journal of Environmental Studies", 15(4A): 177-180.
[11] Berman, B.L., Dietrich, S.S., (eds), 1998, Atlas of photonuclear cross sections obtained with monoenergetic photons., „Atom Data Nucl. Data Tables", 38: 199-338.
[12] National Nuclear Data Center, Brookhaven National Laboratory, web retrieval system, http://www. nndc.bnl.gov/sigma/search.jsp
[13] Firestone, R.B., (eds), 1996, „Table of Isotopes", 8th ed. version 1.0. Lawrence Berkeley National Laboratory, University of California, USA.
[14] Macklin, R.L., Pomerance, H.S., 1955, Resonance capture integrals., „Proc. 1st Intern. Conf. Peaceful Uses Atomic Energy", Geneva, P/833.
[15] Gostkowska B., 2005, Ochrona radiologiczna. Wielkości, jednostki i obliczenia., „Centralne Laboratorium Ochrony Radiologicznej", Warsaw (in Polish).
[16] Price, W.J., 1964, Nuclear Radiation Detection., „USA: McGraw-Hill Book Company".
[17] Facure, A., Falcao, R.C., Silva, A.X., Crispim, V.R., Vitorelli, J.C., 2005, A study of neutron spectra from medical linear accelerators., „Applied Radiation and Isotopes", 62: 69–72.

[18] Esposito,A., Bedogni, R., Lembo, L., Morelli M., 2008, Determination of the neutron spectra around an 18 MV medical LINAC with a passive Bonner sphere spectrometer based on gold foils and TLD pairs., „Radiation Measurements", 43: 1038 – 1043.

[19] Konefał, A., Orlef, A., Dybek, M., Maniakowski, Z., Polaczek-Grelik, K., Zipper, W. 2008, Correlation between radioactivity induced inside the treatment room and the undesirable thermal/resonance neutron radiation produced by linac., „Physica Medica", 24: 212 – 218.

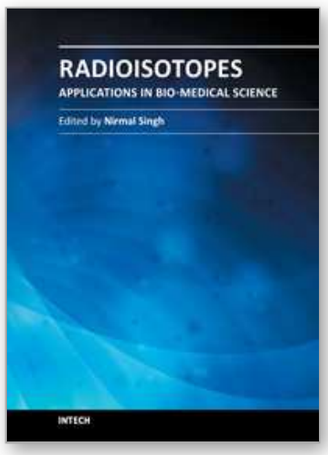

Radioisotopes - Applications in Bio-Medical Science
Edited by Prof. Nirmal Singh

ISBN 978-953-307-748-2
Hard cover, 320 pages
Publisher InTech
Published online 21, November, 2011
Published in print edition November, 2011

The book Radioisotopes - Applications in Bio-Medical Science contains two sections: Radioisotopes and Radiations in Bioscience and Radioisotopes and Radiology in Medical Science. Section I includes chapters on medical radioisotope production, radio-labeled nano-particles, radioisotopes and nano-medicine, use of radiations in insects, drug research, medical radioisotopes and use of radioisotopes in interdisciplinary fields etc. In Section II, chapters related to production of metal PET (positron emission tomography) radioisotopes, 3-dimensional and CT (computed tomography) scan, SS nuclear medicine in imaging, cancer diagnose and treatments have been included. The subject matter will by highly useful to the medical and paramedical staff in hospitals, as well as researchers and scholars in the field of nuclear medicine medical physics and nuclear bio-chemistry etc.

INTECH
open science | open minds

InTech Europe
University Campus STeP Ri
Slavka Krautzeka 83/A
51000 Rijeka, Croatia
Phone: +385 (51) 770 447
Fax: +385 (51) 686 166
www.intechopen.com

InTech China
Unit 405, Office Block, Hotel Equatorial Shanghai
No.65, Yan An Road (West), Shanghai, 200040, China
中国上海市延安西路65号上海国际贵都大饭店办公楼405单元
Phone: +86-21-62489820
Fax: +86-21-62489821

IntechOpen